

Defense Mechanisms Against Training-Hijacking Attacks in Split Learning

Ege Erdoğan, Unat Tekşen, Mehmet Salih Çeliktenyıldız, Alptekin Küpcü, A. Ercüment Çiçek

Abstract—Distributed deep learning frameworks enable more efficient and privacy-aware training of deep neural networks across multiple clients. *Split learning* achieves this by splitting a neural network between a client and a server such that the client computes the initial set of layers, and the server computes the rest. However, this method introduces a unique attack vector for a malicious server attempting to recover the client's private inputs: the server can direct the client model towards learning any task of its choice, e.g. towards outputting easily invertible values. With a concrete example already proposed (Pasquini et al., ACM CCS '21), such *training-hijacking* attacks present a significant risk for the data privacy of split learning clients.

We propose two methods for a split learning client to detect if it is being targeted by a training-hijacking attack or not. We experimentally evaluate our methods' effectiveness, compare them with other potential solutions, and discuss various points related to their use. Our conclusion is that by using the method that best suits their use case, split learning clients can consistently detect training-hijacking attacks and thus keep the information gained by the attacker at a minimum.

Index Terms—Split learning, training-hijacking, privacy-preserving, deep learning.

1 INTRODUCTION

Training deep neural networks (DNNs) requires large amounts of computing power and data; however, relying on a sustained increase in computing power is unsustainable [1], and data from multiple sources cannot always be aggregated (e.g. due to healthcare data regulations [2], [3]).

Distributed deep learning frameworks such as *split learning* (SplitNN) [4], [5] and *federated learning* [6], [7], [8] aim to solve these two problems by allowing a group of data-holders (clients) to train a DNN without raw data sharing. The resulting DNN is effectively trained using the data-holders' collective data.

In federated learning, each client trains a local model and sends its parameter updates to the central server. The server aggregates the parameter updates (e.g. taking their average) of the clients and redistributes the final value. In SplitNN, a DNN is split into multiple parts (typically two); in the two-part setting, clients compute the first few layers of a DNN and send the output to a central server, who then computes the rest of the layers and initiates the backpropagation of gradients. In both methods, no client shares its private data with another party, and all clients end up with the same model.

The Problem. In SplitNN, the server has control over

what the client models learn since the client models' parameter updates are fully determined by the server's backpropagated gradients. This creates a new attack vector we call *training-hijacking*, that has already been exploited in an attack [9], for a malicious server trying to obtain the clients' private data.¹ In the attack, the server leads a client towards outputting values in such a way that it is as easy as possible for the server to obtain back the original inputs from the intermediate values. This is a serious potential violation of the clients' data privacy, but if the clients can detect early in the training process that the server is launching an attack, they can halt training and leave the attacker empty-handed.

Our Solution. Building on our earlier work [10], we propose a set of two methods by which a SplitNN client can detect, without expecting cooperation from the server, if its local model is being hijacked. Our first approach is an active (i.e. clients interfere with the training process) method relying on the empirical observation that if a model is learning the intended classification task, its parameter updates should significantly differ from the norm when the ground truth labels for a batch are randomized. Our second approach is a passive method, demonstrating that a relatively straightforward outlier detection algorithm can reliably detect training-hijacking attacks, albeit at a higher compute cost on the clients' side. We demonstrate our methods' effectiveness through various experiments (using the MNIST [11], Fashion-MNIST [12], and CIFAR10/100 [13] datasets) and discuss different use cases for both.

Our main claim is that both methods can detect an existing attack with perfect accuracy, but the passive method

- Ege Erdoğan and Alptekin Küpcü are with the Department of Computer Engineering, Koç University, 34450 Istanbul, Turkey. E-mail: {eerdogan17, akupcu}@ku.edu.tr
- Unat Tekşen is with the Department of Computer Engineering, Kadir Has University, 34083 Istanbul, Turkey. E-mail: 20181701048@stu.khas.edu.tr
- M. Salih Çeliktenyıldız is with the Department of Electrical and Electronics Engineering, Bilkent University, 06800 Ankara, Turkey. E-mail: m.celiktenyildiz@ug.bilkent.edu.tr
- A. Ercüment Çiçek is with the Department of Computer Engineering, Bilkent University, 06800 Ankara, Turkey, and also with the Computational Biology Department, Carnegie Mellon University, Pittsburgh, 15213 PA, USA. E-mail: cicek@cs.bilkent.edu.tr

Manuscript received MMMM DD, YYYY; revised MMMM DD, YYYY.

¹ By contrast, this attack vector does not exist in federated learning, since the clients can trivially check if their model is aligned with their goals by calculating its accuracy on their local data. Running the same detection method is not possible in split learning since the clients cannot evaluate the model entirely locally.

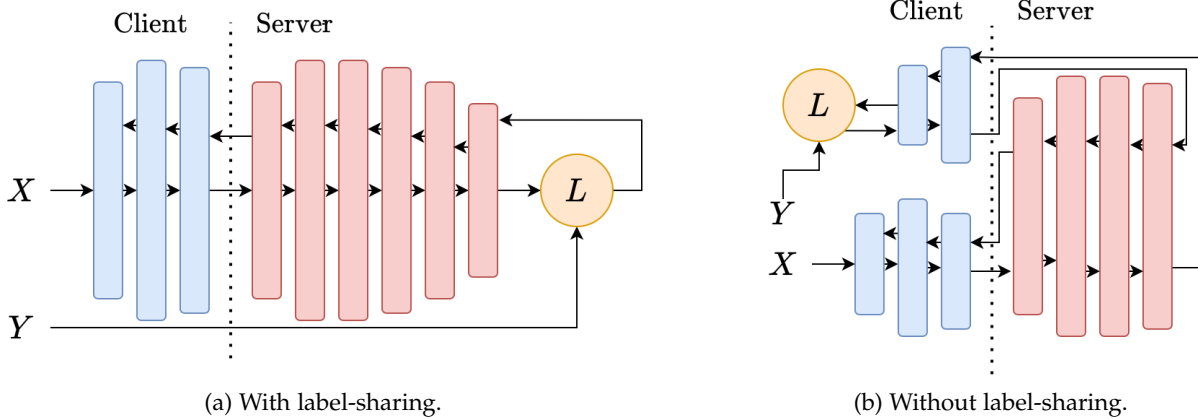


Fig. 1: **Potential SplitNN setups.** Arrows denote the forward and backward passes, starting with the examples X , and propagating backwards after the loss computation using the labels Y . In Figure 1a, clients send the labels to the server along with the intermediate outputs. In Figure 1b, the model terminates on the client side, and the clients do not share their labels.

results in fewer false positives, albeit under stronger assumptions on the clients' capabilities.

The code for our methods is available at <https://github.com/ege-erdogan/splitguard>.

2 BACKGROUND AND RELATED WORK

2.1 Neural Networks

In the context of supervised learning,² a neural network [14] is a parameterized function $f : X \times \Theta \rightarrow Y$ that approximates a function $f^* : X \rightarrow Y$. The training process aims to learn the parameters Θ using a training set consisting of examples \tilde{X} and labels \tilde{Y} sampled from the real-world distributions X and Y .

A typical neural network, also called a *feedforward neural network*, consists of discrete units called *neurons*, organized into layers. Each neuron in a layer takes in a weighted sum of the previous layer's neurons' outputs, applies a non-linear activation function, and outputs the result. The weights connecting the layers to each other constitute the parameters that are updated during training. Considering each layer as a separate function, we can model a neural network as a chain of functions, and represent it as $f(x) = f^{(N)}(\dots(f^{(2)}(f^{(1)}(x)))$, where $f^{(1)}$ corresponds to the first layer, $f^{(2)}$ to the second layer, and $f^{(N)}$ to the final, or the *output* layer. The final layer often has a different activation function, such as the softmax function.

Training a neural network involves minimizing a loss function. However, since the nonlinearity introduced by the activation functions applied at each neuron causes the loss function to become non-convex, we use iterative, gradient-based approaches to minimize the loss function. Since these methods do not provide any global convergence guarantees, it is important that the training data represent the real-world data as accurately as possible.

A widely-used optimization method is *stochastic gradient descent* (SGD). Rather than computing the gradient from the

entire data set, SGD computes gradients for batches selected from the data set. The weights are updated by propagating the error backwards using the backpropagation algorithm. Training a deep neural network generally requires multiple passes over the entire data set, each such pass being called an *epoch*. One round of training a neural network requires two passes through the network: one forward pass to compute the network's output, and one backward pass to update the weights. We will use the terms *forward pass* and *backward pass* to refer to these operations in the following sections. For an overview of gradient-based optimization methods other than SGD, we refer the reader to [15].

2.2 Split Learning

In split learning (SplitNN) [4], [5], [16], a DNN is split between the clients and a server such that each client locally computes the first few layers, and the server computes rest of the layers. This way, a group of clients can train a DNN utilizing, but not sharing, their collective data.

Most of the computational work is offloaded to the server, reducing the cost of training for the clients. However, this partitioning involves a privacy/cost trade-off for the clients, with the outputs of earlier layers leaking more information about the inputs.

Figure 1 displays the two basic setups of SplitNN, the main difference being whether the clients share their labels with the server or not. In Figure 1a, clients compute only the first few layers, and share their labels with the server. The server then computes the loss value, starts backpropagation, and sends the gradients of its first layer back to the client, who then completes the backward pass. The private-label scenario depicted in Figure 1b follows the same procedure, with an additional communication step. Since now the client computes the loss value and initiates backpropagation, it should first feed the server model with the gradient values to resume backpropagation.

The primary advantage of SplitNN compared to federated learning is its lower communication load [17]. While federated learning clients have to share their entire param-

² Supervised learning involves learning through labeled data, as opposed to unsupervised learning, in which the data used is not labeled.

eter updates with the server, SplitNN clients only share the output of a single layer.

SplitNN follows a round-robin training protocol to accommodate multiple clients; clients take turn training with the server using their local data. Before a client starts its turn, it should bring its parameters up-to-date with those of the most recently trained client. There are two ways to achieve this: the clients can either share their parameters through a central parameter server, or directly communicate with each other in a peer-to-peer way.

Choosing a split depth is crucial for SplitNN to actually provide data privacy. If the initial client model is too shallow, an honest-but-curious server can recover the private inputs with high accuracy, knowing only the model architecture (not the parameters) on the clients' side [18]. This implies that SplitNN clients should increase their computational load by computing more layers for better data privacy.

2.3 Training-Hijacking in Split Learning

In a training-hijacking attack against a SplitNN client, the attacker server tries to direct the client models towards its own malicious goal, independent of the actual classification task. The Feature-Space Hijacking Attack (FSHA) (Pasquini et al. CCS '21) [9] is the only proposed training-hijacking attack against SplitNN clients so far. The server aims to lead the clients, by propagating back loss values independent of the original task, towards outputting values in such a way that it is easier to recover the original inputs (clients' private data) than if the model was learning the original task.

In FSHA, the attacker (a SplitNN server) first trains an autoencoder (consisting of the encoder \tilde{f} and the decoder \tilde{f}^{-1}) on some public dataset X_{pub} similar to that of the client's private dataset X_{priv} . It is important for the attack's effectiveness that X_{pub} be similar to X_{priv} . Without such a dataset at all, the attack cannot be launched. The main idea is for the server to bring the output spaces of the client model f and the encoder \tilde{f} as close as possible, so that the decoder \tilde{f}^{-1} can successfully invert the client outputs and recover the private inputs.

After this initial *setup phase*, the client model's training begins. For this step, the attacker initializes a distinguisher model D that tries to distinguish the client's output $f(X_{priv})$ from the encoder's output $\tilde{f}(X_{pub})$. More formally, the distinguisher is updated at each iteration to minimize the loss function.

$$L_D = \log(1 - D(\tilde{f}(X_{pub}))) + \log(D(f(X_{priv}))). \quad (1)$$

Simultaneously at each training iteration, the server directs the client model f towards maximizing the distinguisher's error rate, thus minimizing the loss function.

$$L_f = \log(1 - D(f(X_{priv}))). \quad (2)$$

In the end, the output spaces of the client model and the server's encoder are expected to overlap to a great extent, making it possible for the decoder to invert the client's outputs.

Notice that the client's loss function L_f is totally independent of the training labels, as in changing the value of the labels does not affect the loss function. We will soon refer to this observation.

2.4 Anomaly Detection & Local Outlier Factor

An anomaly detection (AD) method tries to identify data points that are "different" from the "normal," e.g. to identify potentially dubious financial transactions. An important property of an AD method is whether the training data contains outliers or not; if it does, the approach is called *outlier detection*, and otherwise *novelty detection*.

Local outlier factor (LOF) [19], [20], [21] is an unsupervised AD method. It does not make any distribution assumptions and is density-based. Rather than output a binary decision, LOF assigns a *local outlier factor score* to each point, where points in homogeneous clusters have low scores and those with smaller local densities have high scores. The LOF algorithm works as follows:

Using a distance measure d such as the Euclidean distance, calculate the *k-distance* (the distance between a point p and its k^{th} closest neighbor p_k), denoted $d_k(p)$ of each point p . Then calculate its *reachability distance* to each point q as

$$\text{reachDist}(p, q) = \max(d(p, q), d_k(p)),$$

and its *local reachability density* as the inverse of its average reachability distance to its k -neighbors $\text{kNN}(p)$:

$$\text{LRD}(p) = \left(\sum_{q \in \text{kNN}(p)} \frac{\text{reachDist}(p, q)}{k} \right)^{-1}.$$

Finally, assign a LOF score to p as the ratio between the average LRD of its k -neighbors and its own LRD:

$$\text{LOF}(p) = \frac{\sum_{q \in \text{kNN}(p)} \text{LRD}(q)}{k \cdot \text{LRD}(p)}$$

In the end, we expect that if the point p is an inlier, $\text{LOF}(p)$ will be nearly 1 and greater otherwise. Generally, we say p is an outlier if $\text{LOF}(p) > 1$.

Since LOF discovers outliers only based on their local densities and does not try to model the distribution, it does not require us to have even a rough model of the expected outlier behavior which makes it a feasible choice for us.

So far we have not touched upon how k , the number of neighbors, is chosen. There has been methods to choose k automatically and we explain the way we choose k in our study in Section 4.

2.5 Differential Privacy as a Defense Against Training-Hijacking

Differential privacy [22] applied to model training reduces the memorization of individual examples, and thus has been evaluated as a potential defense mechanism against training-hijacking attacks [23], through the clients applying differential privacy on the gradients they receive from the server. As reported in [23], applying DP makes the attack less effective after the same number of iterations compared to the non-DP scenario, but the attacker still obtains high-accuracy results after a higher number of iterations.

Thus, differential privacy by itself does not rule out training-hijacking attacks, the bottom line being as the authors state in [23]: "DP can at most delay FSHA convergence." Nevertheless, this delay can still prove useful. For example, a SplitNN client running one of our methods while

also applying DP on the gradients it receives would have more time to detect a training-hijacking attack before the attacker learns accurate results. DP should not be ruled out as a defense against training-hijacking; in fact, it can be a strong tool for clients when used in the right context.

TABLE 1: Summary of notation and shorthand used throughout the paper.

Notation	
SG-LC	abbrv. SplitGuard Label-Changing
SG-AD	abbrv. SplitGuard Anomaly Detection
P_F	Probability of sending a fake batch
B_F	Share of randomized labels in a fake batch
N	Batch index at which SG-LC starts running
F	Set of fake gradients
R_1, R_2	Random, disjoint subsets of regular gradients
R	$R_1 \cup R_2$
α, β	Parameters of the SG-LC score function
L	Number of classes
A	Model's classification accuracy
A_F	Expected classification accuracy for a fake batch

3 SPLITGUARD: LABEL-CHANGING

3.1 Model Behavior Under a Reversed Task

A supervised learning task can be reversed by randomizing the ground truth values used in training. The points corresponding to high-accuracy classifiers on the parameter space lead to a low classification accuracy when the labels are randomized.

If the client model is learning the intended task, a change should be visible in its parameter updates when the task is reversed. Moreover, since the attacker's objective is independent of the original task, the same discrepancy should not be visible if the server is hijacking the training process. We then need this discrepancy to become evident before the attacker can learn significant amount of information so that the clients can stop training soon enough if the expected discrepancy *does not* occur.

During training with SG-LC, clients intermittently input batches with randomized labels, denoted *fake batches*, as opposed to *regular batches*.³

There are two components of the aforementioned discrepancy between the fake and regular gradients: *angle* and *magnitude*. We make the following two claims (empirically demonstrated in the Supplementary Material):

Claim 1. *If the client model is learning the intended task, then the angle between fake and regular gradients will be higher than the angle between two random subsets of regular gradients (the once-optimal points becomes a point-to-avoid).*⁴

Claim 2. *If the client model is learning the intended task, then fake gradients will have a higher magnitude than regular gradients (fake batches will result in a greater error, resulting in bigger updates).*

³. *Fake gradients* and *regular gradients* similarly refer to the gradients resulting from fake and regular batches.

⁴. Angle between *sets* meaning the angle between the *sums* of vectors in those sets.

Algorithm 1: Client training with SG-LC and the label-sharing SplitNN setup

f, w : client model, parameters
 OPT : optimizer
 P_F : probability of sending fake batches
 B_F : number of labels randomized in fake batches
 N : number of initial batches to ignore
initialize R_1, R_2, F as empty lists
 $\text{rand}(y, B_F)$: randomize share B_F of the labels Y .
before training, set parameters $\alpha, \beta, B_F, P_F, T, N$.
while training do
 for $(x_i, y_i) \leftarrow \text{trainset}$ **do**
 if probability P_F occurs **and** $i \geq N$ **then**
 // sending fake batches
 Send $(f(x_i), \text{rand}(y_i, B_F))$ to server
 Receive gradients ∇_F from server
 Append ∇_F to F
 $\text{MAKE_DECISION}(F, R_1 \cup R_2)$
 // do not update parameters
 else
 // regular training
 Send $(f(x_i), y_i)$ to server
 Receive gradients ∇_R from server
 if $i \geq N$ **then**
 if probability 0.5 occurs **then**
 Append ∇_R to R_1
 else
 Append ∇_R to R_2
 $w \leftarrow w + OPT(\nabla_R)$

3.2 Putting the Claims to Use

At the core of SG-LC, clients compute the SG-LC score, based on the fake and regular gradients they have collected up to that point, and use the scores to detect the attack. We now describe this calculation process in more detail. Table 1 displays the notation we use from here on.

Algorithm 1 explains the modified training procedure in more detail. Starting with the N th batch during the first epoch of training, with probability P_F , clients send fake batches in which the share $B_F \in [0, 1]$ of the labels are randomized. Upon computing the gradient values for their first layer, clients append the fake gradients to the list F , and split the regular gradients randomly into the lists R_1 and R_2 , where $R = R_1 \cup R_2$. To minimize the effect of fake batches on model performance, clients discard the parameter updates resulting from fake batches.

We should first define two quantities. For two sets of vectors A and B , we define $d(A, B)$ as the absolute difference between the average magnitudes of the vectors in A and B :

$$d(A, B) = \left| \frac{1}{|A|} \sum_{a \in A} \|a\| - \frac{1}{|B|} \sum_{b \in B} \|b\| \right|, \quad (3)$$

and $\theta(A, B)$ as the angle between sums of vectors in two sets A and B :

$$\theta(A, B) = \arccos \left(\frac{\bar{A} \cdot \bar{B}}{\|\bar{A}\| \cdot \|\bar{B}\|} \right) \quad (4)$$

where \bar{A} is the sum of the vectors in A . We can restate our two claims more concisely using these quantities under the condition that the client model is learning the intended task:

Claim 1 restated. $\theta(F, R) > \theta(R_1, R_2)$

Claim 2 restated. $d(F, R) > d(R_1, R_2)$

It then follows that if the server is honest, $\theta(F, R) \cdot d(F, R)$ will be greater than $\theta(R_1, R_2) \cdot d(R_1, R_2)$. If the model is learning some other task independent of the labels, then F, R_1 , and R_2 will essentially be three random samples of the set of gradients obtained during training, and it will not be possible to consistently detect the same relationships among them.

To quantify this, after each fake batch, clients compute the value:

$$S = \frac{\theta(F, R) \cdot d(F, R) - \theta(R_1, R_2) \cdot d(R_1, R_2)}{d(F, R) + d(R_1, R_2) + \varepsilon}. \quad (5)$$

The numerator contains the useful information we want to extract, and we divide that result by $d(F, R) + d(R_1, R_2) + \varepsilon$, where ε is a small constant to avoid division by zero, to bound the S value within the interval $[-\pi, \pi]$.

Informally, high S values correspond to an honest server, and low values to a training-hijacking server. For an effective method, we need to define the notions of *higher* and *lower* more clearly. For this purpose, we will define a *squashing function* that maps the interval $[-\pi, \pi]$ to the interval $(0, 1)$, where high S values get mapped infinitesimally close to 1 while the lower values get mapped to considerably lower values. This allows the clients to choose a threshold to consistently separate high and low values.

Our function of choice for the squashing function is the logistic sigmoid function σ . To provide some form of flexibility to the clients, we introduce two hyper-parameters, α and β , and define the function as follows:

$$SG = \sigma(\alpha \cdot S)^\beta \in (0, 1). \quad (\text{SG-LC Score})$$

The function fits naturally for our purposes into the interval $[-\pi, \pi]$, mapping the high-end of the interval to 1, and the lower-end to 0. The parameter α determines the range of values that get mapped very close to 1, while increasing the parameter β punishes the values that are less than 1.

3.3 Detecting the Attack

A client can take into account the *history* of SG-LC scores to make a decision. Although the space of potential decision policies is large, we propose three simple-to-use alternatives (also displayed in Algorithm 2) as follows:

- *Fast*: Fix an early batch index. Report an attack if the last score obtained is less than the decision threshold after that index. The goal of this policy is to detect an attack as fast as possible, without worrying about a high false positive rate.
- *Avg- k* : Report an attack if the average of the last k scores is less than the decision threshold. This policy represents a middle point between the *Fast* and the *Voting* policies.
- *Voting*: Divide the scores sequentially into groups of a fixed size and calculate each group's average. Report attack if the majority of the means is less than the decision

Algorithm 2: Example Detection Policies for SG-LC

```

Function FAST ( $S: scores, T: threshold$ ) :
   $\lfloor$  return  $S[-1] < T$ 

Function AVG-K ( $S: scores, k: number of scores, T: threshold$ ) :
   $\lfloor$  return  $\text{mean}(S[-k :]) < T$ 

Function VOTING ( $S: scores, n: group size, T: threshold$ ) :
  votes = 0
   $c = \lceil \text{len}(scores) / n \rceil$  // group count
  // default  $c = 10$  and  $n = 5$ 
  for  $i$  from 0 to  $c$  do
    group =  $S[i \cdot n : (i + 1) \cdot n]$ 
    if  $\text{mean}(\text{group}) < T$  then
      | votes += 1
  return votes >  $c/2$ 

```

threshold. This policy aims for a high overall success rate (i.e. high true positive and low false positive rates); it can tolerate making decisions relatively later.

4 SPLITGUARD: ANOMALY DETECTION

Our AD-based approach SG-AD consists of two phases: *collecting training data* and *detecting the attack*.

4.1 Collecting Training Data for LOF

We assume the clients have access to the whole neural network architecture (not necessarily the same parameters with the server-side model). They can then train the neural network before the actual training using a portion of their local data to collect a set of *honest* gradients.

This seemingly contradicts the whole reason of using a collaborative ML protocol such as SplitNN: outsourcing computation. However, as we will demonstrate in more detail, clients using a very small share of their local data for the data collection phase still perform accurate detection. Moreover, better data utilization, rather than purely outsourcing computation might be a stronger reason for using SplitNN in certain scenarios (e.g. financially/technologically capable institutions such as universities or hospitals working on regulated private data).

4.2 Detecting the Attack

When the SplitNN training begins, gradients the server sends are input to LOF, and are classified as *honest* (inlier) or *malicious* (outlier). Clients can make a decision after each gradient or combine the results from multiple gradients, by classifying the last few gradients and reaching the final decision by a majority vote between them. If a client concludes that the server is launching an attack, it can stop training and prevent further progress of the attack.

For the LOF algorithm, clients need to decide on a hyperparameter, the number of neighbors. Although there has been work on automatically choosing such values [24], we have observed that setting it equal to one less than the number of honest gradients collected (i.e. the highest

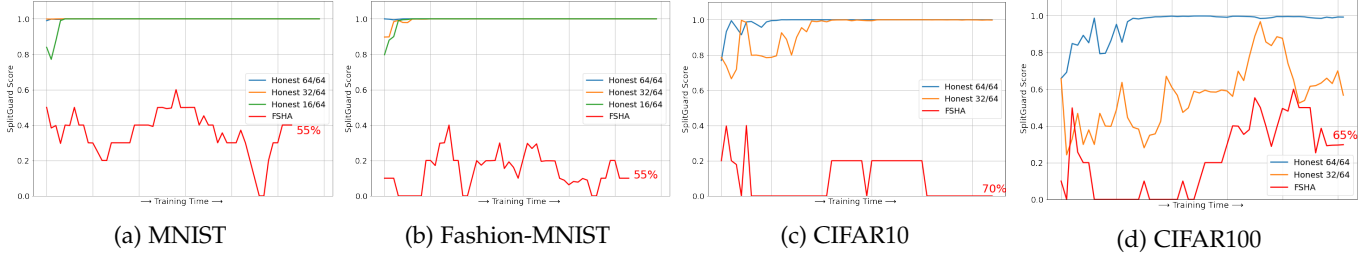


Fig. 2: **SG-LC scores obtained** while training with an honest server, and a FSHA attacker until detection during the first epoch, averaged over 5 runs. The x-axis displays the flow of time during the first epoch. The P_F is set to 0.1, and the B_F values vary when training with an honest server. Lower B_F values are excluded from the CIFAR10/100 results since they do not serve a purpose given the model’s classification accuracy. The labels at the end of FSHA lines correspond to the average detection times as the amount of progress within the first epoch, as shown in Table 2 as well.

Algorithm 3: Client training with SG-AD

f_1, f_2 : client and server models
 f_2^{SIM} : simulated server model
 D : train set size
 n : no. of neighbors for LOF
 w : LOF decision window size
 $\text{train}_{\text{LOF}}$: gradients to train LOF
 pred_{LOF} : gradients for LOF to classify
initialize $\text{train}_{\text{LOF}}$ pred_{LOF} as empty lists
// simulating local model to train LOF
for $(x_i, y_i) \leftarrow \text{train}_{\text{SIM}}$ **do**
 Train f_1 and f_2^{SIM} on (x_i, y_i)
 Append f_1 ’s gradients to $\text{train}_{\text{LOF}}$
// actual SplitNN training with server
for $(x_i, y_i) \leftarrow \text{train}$ **do**
 Send $f_1(x_i)$ and (optional) y_i to the server
 Obtain gradients ∇_1 from the server
 $\text{pred}_{\text{LOF}} \leftarrow \nabla_1$
 Remove older values from pred_{LOF} to keep its size fixed at w .
 if $|\text{pred}_{\text{LOF}}| < w$ **then**
 Continue to next iteration.
 if $\text{LOF}(\text{train}_{\text{LOF}}, n)$ classifies majority of pred_{LOF} as outliers **then**
 Return “attack”.

feasible value) achieves consistently the best performance across all our datasets.

Algorithm 3 explains attack detection process in detail. Before training, clients allocate a certain share of their training data as a separate set $\text{train}_{\text{SIM}}$ and train a local copy of the server-side layers using that dataset. The resulting gradients then constitute the training data of LOF, denoted $\text{train}_{\text{LOF}}$. During the actual training with SplitNN, each gradients received from the server is input to LOF, and classified as an outlier/inlier. With the window size w , clients decide that the server is attacking if at least w LOF decisions has been collected and the majority of them are outliers (i.e. malicious gradients). Similar to SG-LC, training is stopped as soon as an attack is detected.

5 RESULTS

We now test how accurately our two methods can detect FSHA. For our experiments, we use the ResNet architecture [25], trained using Adam [26], on the MNIST [11], Fashion-MNIST [12], and CIFAR10/100 [13] datasets. We implemented our methods in Python (v 3.7) using the PyTorch library (v 1.9) [27]. In all our experiments, we limit our scope only to the first epoch of training.

5.1 Detecting FSHA by SG-LC

5.1.1 Distinguishable Scores

Figure 2 compares the SG-LC scores obtained against a malicious (FSHA) server and an honest server, averaged over 5 runs with a P_F value of 0.1 and varying B_F values.⁵ We set the α and β values to 7 and 1 for all datasets.

The results displayed in Figure 2 indicate that the scores are distinguishable enough to enable detection by the client. Scores obtained against an honest server are very close or equal to 1, while those obtained against a FSHA server do not surpass 0.8, and vary more vigorously. Higher B_F values are more effective. For example, it takes slightly more time for the scores to get fixed around 1 for Fashion-MNIST with a B_F of 4/64 compared to a B_F of 1.

5.1.2 Decision Policies

We now report the detection statistics for the three example policies described earlier, with a threshold value of 0.9.

Table 2 displays the detection statistics for each of these strategies obtained over 100 runs of the first epoch of training against a FSHA attacker and an honest server with a B_F of 1 and P_F of 0.1. For the *Avg-k* policy, we use k values of 10 and 20; this ensures that the policy can run within the first training epoch.⁶ For the *Voting* policy, we set the group size to 5. Finally, we set N , the index at which label-changing starts running, as 20 for MNIST and F-MNIST, 50 for CIFAR10, and 100 for CIFAR100.⁷

5. The B_F values do not affect the SG-LC scores obtained against a FSHA server, since the client’s loss function L_f is independent of the labels, though as we will discuss later there might be strategic reasons for choosing different B_F values.

6. With a batch size of 64, one epoch is equal to 938 batches for MNIST and F-MNIST, and 782 for CIFAR10/100.

7. The models initially behave randomly. We want to exclude those periods from SG-LC.

TABLE 2: **Attack detection statistics using SG-LC and SG-AD**, collected over 100 runs of the first epoch of training with a FSHA attacker and an honest server. The true positive rate (TPR) corresponds to the rate at which SplitGuard succeeds in detecting FSHA. The false positive rate (FPR) corresponds to the share of honest training runs in which SplitGuard mistakenly reports an attack. The t field denotes the average point of detection (as the share of total batches). Boldface highlights the best method for the dataset in terms of reaching perfect (or the highest) accuracy the earliest.

Method	MNIST			F-MNIST			CIFAR10			CIFAR100		
	TPR	FPR	t	TPR	FPR	t	TPR	FPR	t	TPR	FPR	t
LC-Fast	1.0	0.01	0.016	1.0	0.09	0.016	1.0	0.20	0.110	1.0	0.90	0.120
LC-Avg-10	1.0	0	0.140	1.0	0.03	0.140	1.0	0.29	0.200	1.0	0.75	0.140
LC-Avg-20	1.0	0	0.240	1.0	0.01	0.240	1.0	0.21	0.330	1.0	0.45	0.260
LC-Voting	1.0	0	0.550	1.0	0	0.550	1.0	0.02	0.700	1.0	0.11	0.650
AD	1.0	0	0.011	1.0	0	0.011	1.0	0.02	0.013	1.0	0.02	0.014

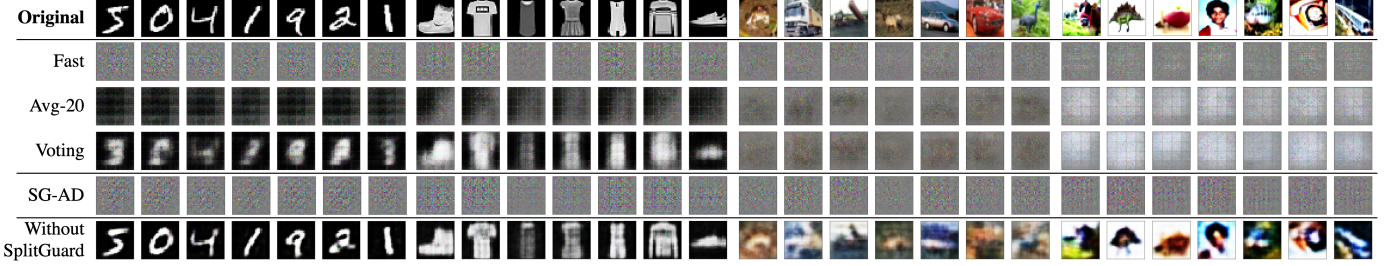


Fig. 3: **Results obtained by a FSHA attacker** for the MNIST, F-MNIST, CIFAR10, and CIFAR100 datasets with respect to the detection times (as shown in Table 2 for SG-LC, and SG-AD) of different methods. The first row displays the original images, and the last row displays the results obtained by a FSHA attacker able to run for an arbitrary duration without being detected.

Most significantly, all the strategies achieve a perfect true positive rate (i.e. successfully detect all runs of FSHA). Expectedly, the *Fast* strategy achieves the fastest detection times as denoted by the t values in Table 2, detecting in at most a hundred training batches all instances of the attack.

False positive rates increase as the model’s accuracy decreases, moving from MNIST to F-MNIST and then to CIFAR10/100. This means that more training time should be taken to achieve higher success rates in more complex tasks. However, as we will observe in Section 5.3, the model not having a high performance also implies that FSHA will be less effective. Nevertheless, the *Voting* policy achieves a false positive rate of 0 for (F-)MNIST, 0.02 for CIFAR10, and 0.11 for CIFAR100, indicating that despite the relatively high false positive rates of the *Fast* and *Avg-k* policies, better detection performance in less time is achievable through more sophisticated policies, such as the *Voting* policy.

5.2 Detecting FSHA with SG-AD

We test the LOF algorithm’s performance when used with different shares of client training data and different decision window sizes using the MNIST [11], F-MNIST [12], and CIFAR10/100 [13] datasets. As stated earlier, we set the number of neighbors to the highest possible value (i.e. one less than the number of training points).

For each configuration, we measure the true and false positive rates by testing the method on 100 randomly-initialized honest and FSHA runs each; a positive (attack detected) decision in a FSHA run is a true positive, and in a honest run a false positive. To make sure we can detect the attack early enough, we start the algorithm after the

required number of gradients for the decision window has been obtained.

Table 2 displays the detection results for the best possible setup (window size 10 and LOF train data rate of 1%), with the more comprehensive results covering a wider range of hyperparameters shown in the Supplementary Material.

In the more simpler MNIST and F-MNIST datasets, our method achieves a TPR of 1 and FPR of 0, meaning it can detect if there is an attack or not with perfect accuracy. For the more complex CIFAR datasets, 2% of honest runs are classified as malicious, but that also reduces to zero as more data is allocated for LOF (Supplementary Material). We should also note that since AD requires a fewer number of gradients to start running (e.g. compared to LC-Voting), it detects the attack considerably faster than LC.

5.3 What Does the Attacker Learn Until Detection?

We now analyze what an FSHA adversary can learn until the detection batch indices displayed in Table 2 for SG-LC, and SG-AD. Figure 3 displays the results the FSHA attacker obtains until it is allowed to run for the respective times.

If stopped very early within the first epoch (e.g. with the *Fast* policy), the attacker obtains not much more than random noise. Furthermore, the attack requires more time to obtain high-fidelity results as the dataset gets more complex. Using CIFAR100, even if the attack is detected in the second half of the epoch (*Voting*), it is difficult to distinguish the attack outputs from each other, let alone compare their similarity to the original inputs. Most importantly, while SG-AD’s FPR values of 0 can be compared to the *Voting* policy, SG-AD detects the attack earlier, meaning the server

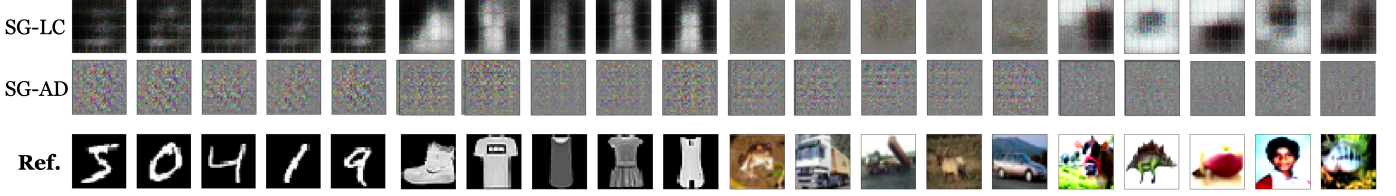


Fig. 4: **Results the FSHA attacker obtains when it performs multitask learning until detection** for the MNIST, F-MNIST, CIFAR10, and CIFAR100 datasets, with 5 images randomly selected from each dataset, until the detection time for the Voting policy for SG-LC and the times shown in table 3 for SG-AD. The bottom row displays the original inputs.

TABLE 3: **Detection results against a server launching FSHA while performing multitask learning** with attack weight 0.5 on the ResNet model for the MNIST and CIFAR datasets, averaged over 100 independent runs for both methods. False positives correspond to the honest server scenario with the results shown earlier in Table 2.

Method	MNIST		F-MNIST		CIFAR10		CIFAR100	
	TPR	<i>t</i>	TPR	<i>t</i>	TPR	<i>t</i>	TPR	<i>t</i>
Fast	1.0	0.015	1.00	0.028	1.00	0.030	1.0	0.140
Avg-10	1.0	0.110	1.00	0.110	1.00	0.140	1.0	0.140
Avg-20	1.0	0.220	1.00	0.220	1.00	0.260	1.0	0.260
Voting	1.0	0.320	1.00	0.310	1.00	0.470	1.0	0.400
AD	1.0	0.012	0.98	0.029	0.98	0.026	1.0	0.064

learns less information compared to when the *Voting* policy is used.

Finally, the CIFAR10/100 results also show that the attacker having more time for a more complex task is tolerable because after the same number of batches, the attacker’s results for MNIST and Fashion-MNIST are more accurate compared to the CIFAR10/100 results.

5.4 Against a Multitasking FSHA Server

As a response to the preceding discussion, the question might arise of the server somehow including the label values in the attack in an attempt to subvert the detection process.⁸ A reasonable way of doing this is to make the client optimize both the FSHA loss and the classification loss functions, e.g. by computing their weighted average, an *attack weight* of 1 meaning plain FSHA and 0 no attack.

Table 3 displays the true positive rates for both our methods against a multitasking server. SG-LC again detects all instances of the attack, but although SG-AD maintains a high TPR of >80% for our recommended setup of 1% AD data rate and 10 window size, it fails to detect some instances of the attack.

Finally, Figure 4 displays the results obtained by a FSHA server performing multitask learning with varying attack weights. A very low attack weight such as 0.01 produces random-looking results, while the distinction between a full- and half-attack result is less clear when compared to the results in Figure 4. However, it is not clear whether this is an inherent property of the attack, or is specific to the dataset or client/server model architectures.

8. This only concerns the shared-label SplitNN setup (Figure 1a) since in the private-label scenario the server does not have access to the label values input to the classification loss.

6 COMPARING SG-AD AND SG-LC

6.1 SG-LC Requires Less Time/Space

Figure 5 compares the time overhead of SG-AD and SG-LC as the share of normal training time incurred as an overhead, averaged over 5 runs across our test datasets.

Since SG-AD involves training the whole model on part of client data, SG-LC’s overhead is lower, less than 10% of the SplitNN training time for all datasets. Furthermore, while reducing the share of client data used to train LOF decreases SG-AD’s overhead, the reduction is not directly proportional to the share of data; e.g. using 1% of client data still results in an additional cost of $\sim 55\%$ for CIFAR100 and $\sim 35\%$ for other datasets.

Space-wise for SG-LC, for each of the sets F , R_1 , R_2 , the clients should store two values: a sum of all vectors in the set, and the average magnitude of the vectors in the set. The former has the dimensions of a single gradient vector, and the latter is a scalar. Since both of these can be maintained in a running way, the space requirement is independent of the time for which SG-LC is run. To run the LOF algorithm on the other hand, the training examples for LOF should be stored for further computation later on. The space requirement grows linearly with the share of client data used in training, as opposed to the constant use of the label-changing method.

SG-AD inevitably incurs a higher cost space- and time-wise on the clients, albeit at a stronger performance as discussed above. Collecting data for LOF requires simulating an epoch from start, and while smaller shares of training data used for this step reduces the overall cost, the reduction is not directly proportional (i.e. using 1% of the data does not make training 100x faster); thus the cost of preparing SG-AD is higher than the overhead incurred by SG-LC during training.

This, combined with the better accuracy of SG-AD makes it a better choice for highly sensitive setups in which clients can tolerate the additional costs.

6.2 Both Achieve High TPR; SG-AD Obtains Lower FPR

Overall, while both methods can achieve a perfect true-positive rate (i.e. detect all instances of the attack) against a server only launching the attack, SG-AD achieves a lower false-positive rate especially for the more complex CIFAR tasks (with window size 10, it achieves an FPR of 0 compared to the minimum 0.02 of SG-LC). This is not surprising, since SG-LC’s decisions rely on the difference between fake and regular gradients, and SG-AD’s decisions rely on the gradients’ similarity to the ground-truth honest gradients

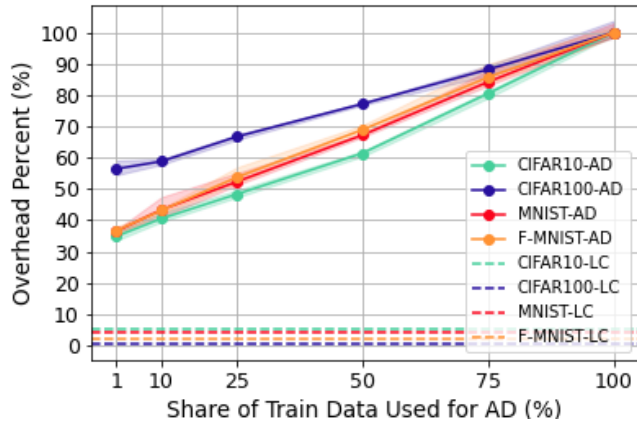


Fig. 5: **Time overhead comparison** between SG-LC and SG-AD, with respect to varying percentage of client data used to train LOF, averaged over 5 runs. The y-axis displays the additional time required as a share of the non-SG training time. Solid lines correspond to SG-AD and the dashed lines represent SG-LC.

obtained during the simulation step. The latter can be said to be a more direct comparison between the actual quantities of interest, while SG-LC compares the outcome of an intervention with the expected outcome.

6.3 SG-AD is Simpler to Use, Requires Fewer Hyperparameters

While SG-AD has a higher cost as discussed above, it is considerably simpler to use. SG-LC involves setting a higher number of parameters, and the process of interpreting the decision is more complex than treating the LOF algorithm as a black-box.

Regarding the choice of hyperparameters for SG-AD, we recommend setting the AD train data rate as low as possible; 1% was enough to reach perfect accuracy in our test scenarios. For the window size, relatively small values such as 10 were enough to reduce the noise in individual decisions and achieve perfect accuracy.

There is a considerably higher number of parameters involved in SG-LC, as can be seen in the first step of the outline in Algorithm 4 adding up to a total of six parameters to choose. While we gave a detailed treatment on choosing and later altering (based on expected/observed behavior of the SG-LC scores) their values in our earlier work [10], we recommend the values we've used in our experiments as reasonable starting points, that is, small α and β values such as 7 and 1, P_F and B_F of 0.1 and 1, and a decision threshold at 0.9. However, we should note (as detailed further in our earlier work) that these parameters also reflect the setup SG-LC is used in; e.g. depending the relative importance of false positives and false negatives.

6.4 Attacker Might Detect SG-LC, but not SG-AD

SG-AD cannot be detected by the server since the client does not diverge from the SplitNN protocol or manipulate its data in any way. However, SG-LC can potentially be

detected by the attacker, especially if the labels are shared too. Then, the attacker can try to circumvent detection by training a legitimate surrogate model for the original task.

If the server controls the model's output (Figure 1a), then it can detect if the loss for a batch is significantly higher than the other ones. Since SG-LC is a potential, albeit not the only, explanation of such behavior, this presents an opportunity for an attacker to detect it. However, the model behaving significantly differently for fake and regular batches also implies that the model is at a stage at which SG-LC is effective. This leads to an interesting scenario: since the attack's and SG-LC's effectiveness both depends on the model learning enough, the attack cannot be detected without the attacker detecting SG-LC and vice versa.⁹

We argue heuristically that this is not the case, due to the clients being in charge of setting the B_F value. For example, with the MNIST dataset for which the model obtains a classification accuracy around 98% after the first epoch of training, a B_F value of 4/64 results in an expected classification accuracy of 91.8% for fake batches. The SG-LC scores on the other hand displayed in Figure 2 being very close to one implies that an attack can be detected with such a B_F value. Thus, clients can make it difficult for an attacker to detect SG-LC by setting the B_F value more smartly, rather than setting it blindly to 1.

Finally, we strongly recommend that a secure SplitNN setup follow the three-part setup shown in Figure 1b to prevent the clients sharing their labels with the server. This way, an attacker would not be able to observe the accuracy of the model, and it would become harder for it to detect SG-LC.

Algorithm 4: SG-LC End-to-End Outline

- 1) Choose parameters $\alpha, \beta, B_F, P_F, N, T$; simulating different server behaviors if possible.
- 2) Choose a decision policy based on user goals (Section 5.1).
- 3) Start training and evaluate scores after each fake batch (Algorithm 1).
- 4) Stop training if the server is likely attacking.

7 CONCLUSION AND FUTURE WORK

We presented two methods for split learning clients to detect if they are being targeted by a training-hijacking attack [9]. When used appropriately (e.g. combined with other defensive tool such as differential privacy), both of our methods demonstrated perfect accuracy in detecting the attack, and reasonable (very low in the case of SG-LC, and zero in the case of SG-AD) false positive rates when there is no attack.

As we have explained in Section 6.4, SG-LC can potentially be detected by the attacker, who can then start sending fake gradients from its legitimate surrogate model and regular gradients from its malicious model. This could again cause a significant difference between the fake and regular gradients, and result in a high SG-LC score. However, a

⁹ Our empirical claim however was that the discrepancy between fake and regular gradients precedes the FSHA server being able to extract useful information.

potential weakness of this approach by the attacker is that now the fake gradients result from two different models with different objectives. Clients might also be able to detect this switch in models. This is another point for which future improvement might be possible.

Another line of future work might involve passive detection of training-hijacking attacks without knowledge of the server-side model architecture. SG-AD requires clients to know the architecture of the entire model so that they can train it with some of their data to obtain training data for LOF. SG-LC does not require such knowledge, and thus can be used in scenarios in which clients do not know the server-side model architecture. A passive method without this architecture assumption would combine the best of both worlds.

Finally, the space of training-hijacking attacks as of this writing is very limited, making it difficult to assess our work's effectiveness against a general class of attacks (e.g. the labels-not-included-in-attack-objective assumption may not always hold as discussed above). As more effort is put into this area (currently covered by [9], [23] and our previous work [10]), it might be possible to develop more sophisticated training-hijacking attacks resistant to label-changing or output gradients less distinguishable from honest gradients.

REFERENCES

- [1] N. C. Thompson, K. Greenewald, K. Lee, and G. F. Manso, "The computational limits of deep learning," *arXiv preprint arXiv:2007.05558*, 2020.
- [2] G. J. Annas, "HIPAA Regulations — A New Era of Medical-Record Privacy?," *New England Journal of Medicine*, vol. 348, pp. 1486–1490, Apr. 2003.
- [3] R. T. Mercuri, "The HIPAA-potamus in health care data security," *Communications of the ACM*, vol. 47, pp. 25–28, July 2004.
- [4] P. Vepakomma, O. Gupta, T. Swedish, and R. Raskar, "Split learning for health: Distributed deep learning without sharing raw patient data," *arXiv preprint arXiv:1812.00564*, 2018.
- [5] O. Gupta and R. Raskar, "Distributed learning of deep neural network over multiple agents," *Journal of Network and Computer Applications*, vol. 116, pp. 1–8, 2018.
- [6] K. Bonawitz, H. Eichner, W. Grieskamp, D. Huba, A. Ingerman, V. Ivanov, C. Kiddon, J. Konečný, S. Mazzocchi, B. McMahan, *et al.*, "Towards federated learning at scale: System design," *Proceedings of Machine Learning and Systems*, vol. 1, pp. 374–388, 2019.
- [7] J. Konečný, H. B. McMahan, D. Ramage, and P. Richtárik, "Federated Optimization: Distributed Machine Learning for On-Device Intelligence," *arXiv:1610.02527 [cs]*, Oct. 2016. arXiv: 1610.02527.
- [8] J. Konečný, H. B. McMahan, F. X. Yu, P. Richtárik, A. T. Suresh, and D. Bacon, "Federated Learning: Strategies for Improving Communication Efficiency," *arXiv:1610.05492 [cs]*, Oct. 2017. arXiv: 1610.05492.
- [9] D. Pasquini, G. Ateniese, and M. Bernaschi, "Unleashing the tiger: Inference attacks on split learning," in *ACM CCS*, pp. 2113–2129, 2021.
- [10] E. Erdogan, A. Küpcü, and A. E. Cicek, "Splitguard: Detecting and mitigating training-hijacking attacks in split learning," in *ACM WPES*, p. 125–137, 2022.
- [11] Y. LeCun, C. Cortes, and C. Burges, "Mnist handwritten digit database," *ATT Labs [Online]. Available: http://yann.lecun.com/exdb/mnist*, vol. 2, 2010.
- [12] H. Xiao, K. Rasul, and R. Vollgraf, "Fashion-mnist: a novel image dataset for benchmarking machine learning algorithms," *arXiv preprint arXiv:1708.07747*, 2017.
- [13] A. Krizhevsky, "Learning multiple layers of features from tiny images," *Master's thesis, University of Toronto*, 2009.
- [14] I. Goodfellow, Y. Bengio, and A. Courville, *Deep Learning*. MIT Press, 2016. <http://www.deeplearningbook.org>.
- [15] S. Ruder, "An overview of gradient descent optimization algorithms," *arXiv:1609.04747 [cs]*, June 2017. arXiv: 1609.04747.
- [16] P. Vepakomma, T. Swedish, R. Raskar, O. Gupta, and A. Dubey, "No peek: A survey of private distributed deep learning," *arXiv preprint arXiv:1812.03288*, 2018.
- [17] A. Singh, P. Vepakomma, O. Gupta, and R. Raskar, "Detailed comparison of communication efficiency of split learning and federated learning," *arXiv preprint arXiv:1909.09145*, 2019.
- [18] E. Erdogan, A. Küpcü, and A. E. Cicek, "Unsplit: Data-oblivious model inversion, model stealing, and label inference attacks against split learning," in *ACM WPES*, p. 115–124, 2022.
- [19] M. M. Breunig, H.-P. Kriegel, R. T. Ng, and J. Sander, "Lof: identifying density-based local outliers," in *ACM SIGMOD*, pp. 93–104, 2000.
- [20] S. Chen, W. Wang, and H. van Zuylen, "A comparison of outlier detection algorithms for its data," *Expert Systems with Applications*, vol. 37, no. 2, pp. 1169–1178, 2010.
- [21] J. H. Janssens, I. Flesch, and E. O. Postma, "Outlier detection with one-class classifiers from ml and kdd," in *2009 International Conference on Machine Learning and Applications*, pp. 147–153, IEEE, 2009.
- [22] C. Dwork, A. Roth, *et al.*, "The algorithmic foundations of differential privacy," *Found. Trends Theor. Comput. Sci.*, vol. 9, no. 3–4, pp. 211–407, 2014.
- [23] G. Gawron and P. Stubbings, "Feature space hijacking attacks against differentially private split learning," *Third AAAI Workshop on Privacy-Preserving Artificial Intelligence*, 2022.
- [24] Z. Xu, D. Kakde, and A. Chaudhuri, "Automatic hyperparameter tuning method for local outlier factor, with applications to anomaly detection," in *2019 IEEE International Conference on Big Data (Big Data)*, pp. 4201–4207, IEEE, 2019.
- [25] K. He, X. Zhang, S. Ren, and J. Sun, "Deep residual learning for image recognition," in *Proceedings of the IEEE conference on computer vision and pattern recognition*, pp. 770–778, 2016.
- [26] D. P. Kingma and J. Ba, "Adam: A Method for Stochastic Optimization," *arXiv:1412.6980 [cs]*, Jan. 2017. arXiv: 1412.6980.
- [27] A. Paszke, S. Gross, F. Massa, A. Lerer, J. Bradbury, G. Chanan, T. Killeen, Z. Lin, N. Gimelshein, L. Antiga, A. Desmaison, A. Kopf, E. Yang, Z. DeVito, M. Raison, A. Tejani, S. Chilamkurthy, B. Steiner, L. Fang, J. Bai, and S. Chintala, "Pytorch: An imperative style, high-performance deep learning library," in *NeurIPS*, pp. 8024–8035, 2019.